Journal of Knot Theory and Its Ramifications
Vol. 35, No. 2 (2026) 2340024 (21 pages)

DOI: 10.1142/S0218216523400242

World Scientific
www.worldscientific.com

A new framework for the Jones polynomial of fluid knots

Renzo L. Ricca*

Department of Mathematics and Applications,
Università degli Studi di Milano-Bicocca,
Via Cozzi 55, 20125 Milano, Italy

Faculty of Science, Beijing University of Technology,
100 Pingleyuan, Beijing 100124, P. R. China
renzo.ricca@unimib.it

Xin Liu

Institute of Theoretical Physics,
Beijing University of Technology, 100 Pingleyuan,
Beijing 100124, P. R. China
xin.liu@bjut.edu.cn

Received 24 December 2022
Revised 25 March 2023
Accepted 26 March 2023
Published 6 July 2023

ABSTRACT

Here we illustrate how Jones' polynomials are derived from the kinetic helicity of vortical flows, and how they can be used to measure the topological complexity of fluid knots by numerical values. Relying on this new findings, we show how to use our adapted Jones polynomial in a new framework by introducing a knot polynomial space whose discrete points are the adapted Jones polynomials of fluid knots, interpreting the topological simplification associated with the natural decay of reconnecting fluid knots as geodesic flows on this space.

Keywords: Topological fluid mechanics; helicity; vortex knots and links; Jones polynomial; knot polynomial space.

Mathematics Subject Classification 2020: 76B47, 57K14, 57M99, 53E99

1. Topological Interpretation of Fluid Helicity in Terms of Linking Numbers and Crossing Signs

A central task of topological fluid mechanics is to determine the relation between topological invariants of fluid structures, such as vortex knots and links, and their dynamics and energy contents. This search started long time ago with Kelvin's vortex atom theory [40], and his ambitious aim to provide a mathematical

*Corresponding author.

justification for the observed discrete energy spectra of chemical elements. We had to wait for another 100 years, with the seminal work of Moffatt [24], to realize that one of the most fundamental conserved quantities of ideal fluid mechanics, i.e. the helicity of fluid flows, admits topological interpretation. In 1984 Berger and Field [5] made further progress considering the decomposition of magnetic helicity of a finite number of isolated flux tubes in terms of the geometry and topology of the constituent field lines. The study of the topological implications of helicity, and its relation to energy, are now a central topic of modern research in fluid mechanics [25, 38, 44]. In this sense topological fluid mechanics represents the first example of a true, topological field theory [1, 29].

For vortical flows in an unbounded, simply connected domain of $\mathbb{R}^3$ kinetic helicity is defined [27, 37] by the volume integral

$$H = \int_V \boldsymbol{u} \cdot \boldsymbol{\omega} \, \mathrm{d}^3\boldsymbol{x}, \tag{1}$$

where $\boldsymbol{u}$ is the velocity, and $\boldsymbol{\omega} = \nabla \times \boldsymbol{u}$ the vorticity in the fluid volume V. Magnetic helicity is defined similarly by replacing $\boldsymbol{u}$ with the magnetic vector potential $\boldsymbol{A}$, and $\boldsymbol{\omega}$ with the magnetic field $\boldsymbol{B}$. In the case of incompressible flows, we have also the supplementary condition $\nabla \cdot \boldsymbol{u} = 0$. Moreau [27] was the first to prove the conservation of the helicity (1) under diffeomorphisms of the background flow maps in V.

Considering the divergence-free $\boldsymbol{\omega}$ as the observable gauge field, we can interpret the velocity field $\boldsymbol{u}$ given by the Biot–Savart formula

$$\boldsymbol{u}(\boldsymbol{x}) = \int_V \frac{\boldsymbol{\omega}(\boldsymbol{x}') \times (\boldsymbol{x} - \boldsymbol{x}')}{|\boldsymbol{x} - \boldsymbol{x}'|^3} \, \mathrm{d}^3\boldsymbol{x}' \tag{2}$$

as a gauge potential. Hence, Eq. (1) being a functional integral of $\boldsymbol{\omega}$ (see [1, Theorem 1.15]) can be interpreted as a global, physical observable. Moreau's proof of the conservation of kinetic helicity in ideal fluid mechanics can thus be recast in the following:

Theorem 1.1 ([1]). *Let $\boldsymbol{\omega}$ be a divergence-free vector field defined on a manifold $\mathcal{M}$. The helicity integral* (1) *is conserved under any arbitrary, volume-preserving diffeomorphism of $\mathcal{M}$.*

It is interesting to note that well before Moreau's proof of the invariance of H in fluid mechanics, it was Whitehead [42] who recognized (in 1946!) the topological character of Eq. (1), by interpreting H as Hopf invariant.

1.1. *Helicity in terms of linking numbers*

When the vorticity field is localized in flux tubes made of a bundle of vortex lines running parallel to the tube axis (no flux through the tube boundary), Eq. (1) admits interpretation in terms of linking numbers. For thin flux tubes forming knots and links in an ideal fluid (no dissipation or resistive effects) computation of

> … Ce n'est évidemment pas le cas général; comme exemple d'îlot ayant un H non nul, nous proposons un système de deux anneaux tourbillonnaire de révolution, d'intensité respectives I_1 et I_2, *enlacés*, le tout plongé dans du fluide irrotationnel pour constituer un îlot D simplement connexe : on trouve alors $H = 2\, I_1\, I_2$.
>
> … Evidently this is not the general case; as an example of a sub-region that has a non-zero H, we propose a system of two vortex rings, respectively of strength I_1 and I_2, *linked*, the whole embedded in an irrotational fluid to form a simply connected region: thus we obtain $H = 2\, I_1\, I_2$.

Fig. 1. (Top) In a footnote to his paper on the conservation of helicity [27, p. 2812, footnote 1] Moreau considers the case of two linked vortex rings, anticipating (without proof) the correct value of helicity; (bottom) English translation.

the kinetic helicity simplifies. In a footnote to his paper (see Fig. 1) Moreau [27] considers the case of two linked vortices, anticipating without proof the correct result later proved by Moffatt in 1969 (see below). The demonstration that the helicity integral can indeed be expressed in terms of the linking number was given by Moffatt [24], and then extended by Moffatt and Ricca [26, 33] to include self-linking. In the case of an N-component link $\mathcal{L} = \bigsqcup_{i=1}^{N} \mathcal{K}_i$, where each $\mathcal{K}_i$ is a vortex tube of flux Φ_i, we have

Theorem 1.2 ([24, 26]). *The helicity of a vortex link $\mathcal{L}$ is given by*

$$H(\mathcal{L}) = \sum_{i \neq j} \Phi_i \Phi_j Lk_{ij} + \sum_{i=j} \Phi_i^2 Sl_i, \tag{3}$$

where $Lk_{ij} \equiv Lk(\mathcal{K}_i, \mathcal{K}_j)$ is Gauss' linking number of $\mathcal{K}_i$ and $\mathcal{K}_j$, and $Sl_i \equiv Sl(\mathcal{K}_i)$ is the Călugăreanu–White self-linking number of $\mathcal{K}_i$.

A sketch of the proof is shown in Fig. 2, where the first sum in (3) is referred to as mutual helicity H_{mutual}, and the second sum as self-helicity H_{self}. Evidently,

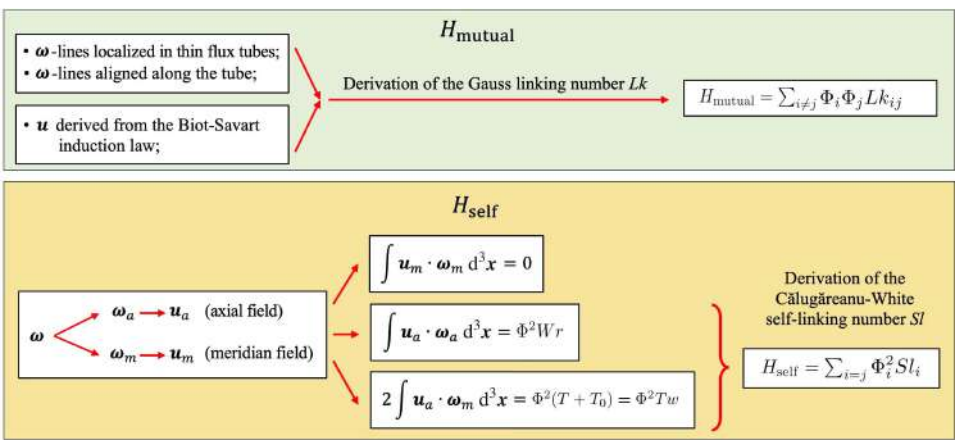

Fig. 2. Scheme of the proof of H_{mutual} [24], and of H_{self} [26].

when $\Phi_1 = \cdots = \Phi_N = \Phi$ (a typical situation for quantum vortex defects) Eq. (3) simplifies further, taking the form

$$H(\mathcal{L}) = \Phi^2 \left(\sum_{i \neq j} Lk_{ij} + \sum_{i=j} Sl_i \right). \tag{4}$$

1.2. *Helicity computation in terms of crossing signs*

It is useful to recall that the self-linking number Sl is a topological invariant of a framed knot, and it admits decomposition according to the fundamental formula [6, 41]

$$Sl = Wr + Tw, \tag{5}$$

where Wr denotes the writhing number, and Tw the total twist number (sum of the normalized total torsion T and intrinsic twist T_0), all global geometric quantities of the framed knot. Since the computation of the volume integral (1) is rather difficult, Eq. (3) provides a remarkable simplification in terms of measurable quantities, quite convenient for theoretical progress and practical applications. By identifying the tube centerline with the knot, a particularly useful approach to compute mutual linking and writhing number is offered by the algebraic interpretation of these quantities in terms of signed crossings [34, 35]. According to the sign convention of Fig. 3(a), we have

$$Lk(\mathcal{K}_i, \mathcal{K}_j) = \frac{1}{2} \sum_{r \in \{\mathcal{K}_i \sqcap \mathcal{K}_j\}} \varepsilon_r, \quad Wr(\mathcal{K}_i) = \left\langle \sum_{r \in \{\mathcal{K}_i \sqcap \mathcal{K}_i\}} \varepsilon_r \right\rangle, \tag{6}$$

where $\{\mathcal{K}_i \sqcap \mathcal{K}_j\}$ and $\{\mathcal{K}_i \sqcap \mathcal{K}_i\}$ denote, respectively, the set of apparent intersections of the tube centerlines of $\mathcal{K}_i$ and $\mathcal{K}_j$, and of self-intersections of $\mathcal{K}_i$ given by the indented link projections; angular brackets denote averaging over all directions of projection. An elementary example of the linking computation for a pair of loops by the left-hand side formula of (6) is shown in Fig. 3. The right-hand side formula for the writhing number Wr above is exact, but the theoretical value can be approximated by estimating Wr through a finite number of projections. Direct application

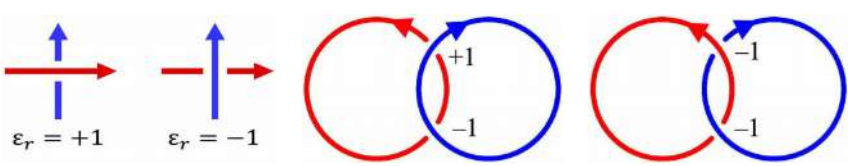

(a) (b) (c)

Fig. 3. (a) Algebraic crossing sign convention; (b) indented diagram of a 2-component unlink ($Lk = 0$); (c) indented diagram of the negative Hopf link ($Lk = -1$).

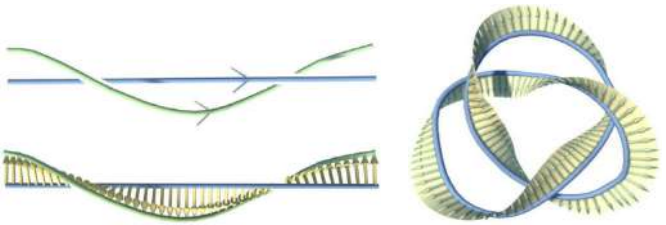

(a) (b)

Fig. 4. (Color online) Knot framing is given by the mathematical ribbon (visualized by small, yellow arrows) prescribed on the knot: (a) twist is visualized by the uniform rotation of the flux tube field lines with respect to the ribbon around the knot centerline (blue curve); (b) a framed trefoil (pictures taken from [12]).

of this simple technique has proven to be accurate, even when only three mutually orthogonal projections are considered [3]. The two contributions left out from the computation of Sl are the total torsion and the intrinsic twist. Total torsion T is given by the geometry of the knot, and because it involves third derivatives of the arc-length, its contribution is generally rather modest (amounting to just a few percentages of the total Sl); thus, to a first approximation it can be ignored.

The intrinsic twist T_0 of a physical knot is, in general, very hard to compute. It is given by the uniform rotation of the field lines with respect to the knot framing (see Fig. 4). For an approximated estimate of total helicity we can thus rely on diagram projections to get

$$H(\mathcal{L}) \approx \Phi^2 \left(\frac{1}{2} \sum_{r \in \{\mathcal{K}_i \sqcap \mathcal{K}_j\}} \varepsilon_r + \left\langle \sum_{r \in \{\mathcal{K}_i \sqcap \mathcal{K}_i\}} \varepsilon_r \right\rangle_{\perp} \right), \tag{7}$$

where $\langle \ldots \rangle_{\perp}$ denotes estimated averaging over mutually orthogonal projections. From direct numerical simulations of fluid flows, however, helicity can be computed straightforwardly by its integral definition through (1). In this case, we can estimate total twist by the combined use of (1) and (7), to get

$$Tw(\mathcal{L}) = \int_V \boldsymbol{u} \cdot \boldsymbol{\omega} \mathrm{d}^3\boldsymbol{x} - \Phi^2 \left(\frac{1}{2} \sum_{r \in \{\mathcal{K}_i \sqcap \mathcal{K}_j\}} \varepsilon_r + \left\langle \sum_{r \in \{\mathcal{K}_i \sqcap \mathcal{K}_i\}} \varepsilon_r \right\rangle_{\perp} \right). \tag{8}$$

This information is quite useful to take account of the energy transfers of interacting flux tubes.

2. Helicity as an Abelian Chern–Simons Action

Topological information based purely on linking numbers has a well-known limitation, due to the limited ability of linking numbers to detect topologically different

(a) (b) (c)

Fig. 5. (a) 3 unlinked circles, (b) 3-component link forming the Borromean rings, and (c) the Whitehead link; regardless of their different topologies, all these link types share the same zero linking number.

link types. The three cases considered in Fig. 5 demonstrate the failure of the linking number to detect different topologies. Evidently, any helicity computation based purely on linking numbers will suffer from this limitation. As we know, more powerful topological information comes from knot polynomials. In order to introduce these invariants in topological fluid mechanics, it is useful to re-consider helicity in a new setting.

In the language of exterior differential forms, the velocity field is a 1-form $u = u_i \mathrm{d}x^i$, with the 2-form given by $\mathrm{d}u = \frac{1}{2}\partial_i u_j \mathrm{d}x^i \wedge \mathrm{d}x^j$ ($\wedge$ denoting wedge product). Vorticity is also a 1-form, defined by the Hodge dual $\omega = *\mathrm{d}u$, i.e. $\omega = \omega_i \mathrm{d}x^i = (\epsilon_i{}^{jk}\partial_j u_k)\mathrm{d}x^i$. The helicity integral (1) can thus be written as a 3-form, given by

$$H = \int_V u \wedge \mathrm{d}u. \tag{9}$$

In this form, the integral above can be recognized as an Abelian Chern–Simons (CS) action. Generally speaking, a CS action S_{CS} with a generic, non-Abelian group G is given by

$$S_{\mathrm{CS}} = \frac{k}{4\pi}\int_{\mathcal{M}} \mathrm{CS}(A) = \frac{k}{4\pi}\int_{\mathcal{M}} \left(A \wedge dA + \frac{2}{3} A \wedge A \wedge A \right), \tag{10}$$

where $k/4\pi \in \mathbb{R}$ is a (level) parameter, $\mathrm{CS}(A)$ the so-called CS 3-form, $A = A(x)$ a connection 1-form on the principal G-bundle (i.e. a gauge potential); $A = A_i^a T_a \mathrm{d}x^i$, with $\{T_a\}$ ($a = 1, \ldots, \dim(G)$) are the generators of G, and $\{x^i\}$ ($i = 1, 2, 3$) the coordinates of the 3-dimensional base manifold $\mathcal{M}$. When G is non-Abelian (the generic case) $[T_a, T_b] \neq 0$, and the cubic term $A \wedge A \wedge A$ does not vanish. But in the special case of $G = U(1)$ (Abelian group) the cubic term in (10) vanishes, so that

$$S_{\mathrm{CS}} = \frac{k}{4\pi}\int_V A \wedge \mathrm{d}A. \tag{11}$$

By setting the prefactor $k/4\pi = 1$ the integral CS 3-form can be identified with (9), by interpreting A as the velocity field u (cf. the London relation in

superconductivity [11]). Kinetic helicity can thus be seen as a special Abelian case of the CS action (10).

Following the work of Witten, CS theory has become the benchmark of a topological quantum field theory (TQFT). As shown by Witten [43], the global, physical observables of the CS theory are given by the Wilson loops represented by knots in a 3-dimensional spacetime. Their values are computed by knot polynomial invariants that generalize the celebrated Jones polynomial [14]. A physical interpretation of these invariants comes from the TQFT description of the CS path integrals. These are defined as the vacuum expectation values of the Wilson loops, according to the expression

$$\left\langle \prod_i \mathrm{e}^{\mathrm{i} \oint_{\mathcal{K}_i} A} \right\rangle = \frac{1}{Z} \int [\mathcal{D}A] \big(\mathrm{e}^{\mathrm{i} \sum_i \oint_{\mathcal{K}_i} A}\big) \mathrm{e}^{\mathrm{i} 2\pi S_{\mathrm{CS}}}. \tag{12}$$

Wilson loops are gauge invariant functionals that arise from the parallel transport of the gauge field A along closed loops given by the knots $\mathcal{K}_i$ $(i = 1, \ldots, N)$, and they are represented in (12) by the expression $\exp(\mathrm{i} \sum_i \oint_{\mathcal{K}_i} A)$. The term $[\mathcal{D}A]$ denotes functional integration performed on A, and Z a partition function that plays the role of a normalization constant. By replacing the potential A with the velocity u the CS action (11) (appropriately re-scaled) becomes the helicity integral; substituting this expression into the integrand of (12), we have

$$\big(\mathrm{e}^{\mathrm{i} \sum_i \oint_{\mathcal{K}_i} u}\big) \mathrm{e}^{\mathrm{i} \int_V u \wedge \mathrm{d}u} = \big(\mathrm{e}^{\mathrm{i} \sum_i \oint_{\mathcal{K}_i} u}\big) \mathrm{e}^{\mathrm{i} H}. \tag{13}$$

Now let us go back to vortex knots. Since we consider fields localized in thin flux tubes, we can take $\boldsymbol{\omega} = \omega_0 \hat{\boldsymbol{t}}$, with ω_0 constant and $\hat{\boldsymbol{t}}$ unit tangent to the tube centerline, and reduce the volume integral (1) to a line integral given by the field line helicity [4, 36]

$$H = \sum_i \Phi_i \oint_{\mathcal{K}_i} \boldsymbol{u} \cdot \mathrm{d}\boldsymbol{l}, \tag{14}$$

where as usual Φ_i (constant) denotes the flux of vorticity, and $\mathrm{d}\boldsymbol{l}$ the elementary unit length along the knot $\mathcal{K}_i$. Total helicity H is thus reduced to a sum of line integrals along $\mathcal{K}_i$ [3]. For simplicity, we can take $\Phi_i = \Phi = 1$, so we have $H = \sum_i \oint_{\mathcal{K}_i} u$, where u denotes the Biot–Savart velocity 1-form. By substituting this line integral into (13), we have

$$\big(\mathrm{e}^{\mathrm{i} \sum_i \oint_{\mathcal{K}_i} u}\big) \mathrm{e}^{\mathrm{i} H} = f\big(\mathrm{e}^{\mathrm{i} \oint_{\mathcal{K}_i} \boldsymbol{u} \cdot \mathrm{d}\boldsymbol{l}}\big), \tag{15}$$

function of e^H only (in terms of the field line helicity). In the present approach, the path-ordering integral formalism can be dropped (not being necessary for an Abelian theory), so that we can proceed with the derivation of the knot polynomials from the field line functional e^H.

3. Physical Heuristics for Deriving the Jones and HOMFLYPT Polynomials from Helicity

Here we present a concise review of the work done by Liu and Ricca in 2012 and 2015 to derive and apply Jones and HOMFLYPT knot polynomials of classical knot theory to topological fluid mechanics. A knot polynomial is an invariant $Q = Q(\mathcal{K}; \xi_i)$ which assigns to each knot or link $\mathcal{K}$ a Laurent polynomial in one or more variables ξ_i $(i = 1, 2, \ldots)$ with integer coefficients. Since the field line helicity (14) and the knot polynomial are invariants under an ideal flow map φ, any diffeomorphic deformation of $\mathcal{K}$ leaves H and Q invariant. For vortex knots, the polynomial variables ξ_i play the role of gauge scalar quantities, so that the invariance of Q requires the vanishing covariant derivative (and parallel transport) of ξ_i under φ, along $\mathcal{K}$ and in time. In the present context, a gauge covariant derivative is a Lagrangian derivative, so that for each $\boldsymbol{u}$ we must have (see [9], Eqs. (33)–(34) replacing $\boldsymbol{A}$ with $\boldsymbol{u}$)

$$\frac{\mathrm{d}\varphi(\xi_i)}{\mathrm{d}s} = (\boldsymbol{u} \cdot \nabla_s \boldsymbol{x})\varphi(\xi_i) = (\boldsymbol{u} \cdot \hat{\boldsymbol{t}})\varphi(\xi_i) \quad (i = 1, 2, \ldots), \tag{16}$$

where s is some parameter along the knot centerline, and $\nabla_s \boldsymbol{x} = \mathrm{d}\boldsymbol{x}/\mathrm{d}s = \hat{\boldsymbol{t}}$ is the unit tangent to $\mathcal{K}$. Thus, under appropriate re-scaling direct integration of (16) from some initial to some final state gives $\varphi_1 = \varphi_0(\xi_i)$, with

$$\xi_i = \mathrm{e}^{\oint_{\mathcal{K}} \boldsymbol{u}\cdot\hat{\boldsymbol{t}}\,\mathrm{d}s} = \mathrm{e}^{\oint_{\mathcal{K}} \boldsymbol{u}\cdot\mathrm{d}\boldsymbol{l}} \quad (i = 1, 2, \ldots). \tag{17}$$

A fluid knot $\mathcal{K}$ has orientation inherited by the constituent field lines. Denoting by  the oriented unknot, and by  ,  and  the overcrossing, undercrossing and smoothing of the distinguished crossing site in the knot diagram D, we have [14].

Definition 3.1. The Jones polynomial $V(\mathcal{K}) = V(\mathcal{K}; t)$ of the oriented knot $\mathcal{K}$ in the single parameter t is defined by

$$\text{(i)}: \quad V(\,\text{  }\,) = 1\,, \tag{18}$$

$$\text{(ii)}: \quad t^{-1}V(\,\text{  }\,) - tV(\,\text{  }\,) = (t^{1/2} - t^{-1/2})V(\,\text{  }\,)\,. \tag{19}$$

Direct application of the skein relation above gives the Jones polynomial of knots and links [15]. Using (17) above, we can prove the following result:

Theorem 3.2 ([19]). *Let $H = H(\mathcal{K})$ be the helicity of a physical, framed knot $\mathcal{K}$. Then*

$$\mathrm{e}^{H(\mathcal{K})} = \mathrm{e}^{\oint_{\mathcal{K}} \boldsymbol{u}\cdot\mathrm{d}\boldsymbol{l}}, \tag{20}$$

appropriately re-scaled, satisfies (with a plausible statistical hypothesis) the skein relation of the Jones polynomial $V = V(\mathcal{K})$.

For details of the proof, see [19, 30]. The derivation is outlined in Fig. 6, where we make two assumptions; (i) since vortex knots are naturally led to interact and

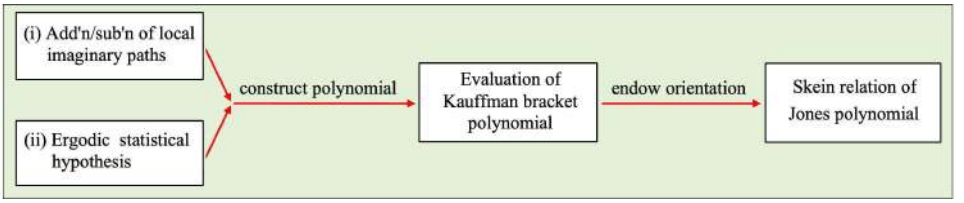

Fig. 6. Scheme of the proof of Theorem 3.2 according to [19].

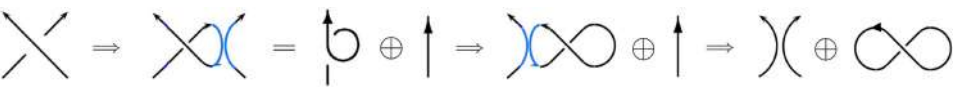

Fig. 7. (Color online) Crossing state decomposition by addition and subtraction of "imaginary paths" (blue online); note the interpretation of the crossing state in terms of the closed curl.

reconnect locally, in analogy with the theory of particle interactions we assume that reconnection events can be described by a virtual operation of addition and subtraction of vortex strands (interpreted mathematically as "imaginary paths"), according to the scheme of Fig. 7. Hence, each unoriented crossing state admits the following hypothetical decomposition:

(21)

(22)

One then proceeds to encode the decompositions above into the evaluation of the Kauffman bracket polynomial for unoriented knots [15], i.e.

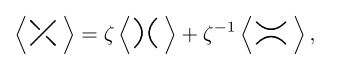

(23)

where ζ (the bracket variable) is also a ξ-variable obeying Eq. (17). (ii) We also assume (statistical hypothesis) that the two decompositions above have equal probability to occur (cf. [10, Wick's Theorem, p. 158]), noting that the subsequent strand orientation breaks the 90° rotational symmetry of these decompositions, thus entailing an ergodic assumption.

For physical applications, we can relate the Jones single variable t with the helicity $H(\mathcal{K})$; considering vortex knots as zero-framed knots, writhe and twist are interlocked by the zero helicity condition (as for vortex defects in condensed matter physics) $Sl = Wr + Tw = 0$. By identifying (say) writhe with the t variable, we can take, for example

$$t^{1/2} = \mathrm{e}^{H} = \mathrm{e}^{\lambda_\omega W r}, \tag{24}$$

where $\lambda_\omega \in [0, 1]$ represents the uncertainty associated with the directional writhe. From direct measurements, or estimates, of the average writhe $\langle Wr \rangle$ we can then

associate a numerical value to the topology of fluid knots, given by the adapted Jones polynomial.

Following a similar strategy, we can extend this approach to derive from the helicity $H(\mathcal{K})$ the 2-variable HOMFLYPT polynomial $P(\mathcal{K}) = P(\mathcal{K}; a, z)$ in the parameters a and z [13, 28]. We have

Theorem 3.3 ([20]). *Let $H = H(\mathcal{K})$ be the helicity of a physical knot $\mathcal{K}$. Then*

$$\mathrm{e}^{H(\mathcal{K})} = \mathrm{e}^{\oint_{\mathcal{K}} \boldsymbol{u}\cdot \mathrm{d}\boldsymbol{l}}, \tag{25}$$

appropriately re-scaled, satisfies (with a plausible statistical hypothesis) the skein relation of the HOMFLYPT polynomial $P = P(\mathcal{K})$.

The derivation in this case is more elaborate. Since HOMFLYPT is a two-variable polynomial, it cannot be derived directly from the one-variable bracket evaluation, and it is here that the two distinct paths, denoted by Steps 1 and 2 in Fig. 8, come into play. In this heuristic, we first observe that the regular isotopy version of the HOMFLYPT polynomial is determined by the following equations:

$$\text{(i)}: \quad R(\bigcirc) = 1\,, \tag{26}$$

$$\text{(ii)}: \quad R(\text{⟳}) = aR(\uparrow)\,, \qquad R(\text{⟲}) = a^{-1}R(\uparrow)\,, \tag{27}$$

$$\text{(iii)}: \quad R(\times) - R(\times) = zR(\,)(\,)\,, \tag{28}$$

where ⟳ denotes the Reidemeister twist move. By applying (28) to Eqs. (27), we have

$$R\left(\text{⟳}\right) - R\left(\text{⟲}\right) = aR(\uparrow) - a^{-1}R(\uparrow) = zR(\uparrow\bigcirc)\,, \tag{29}$$

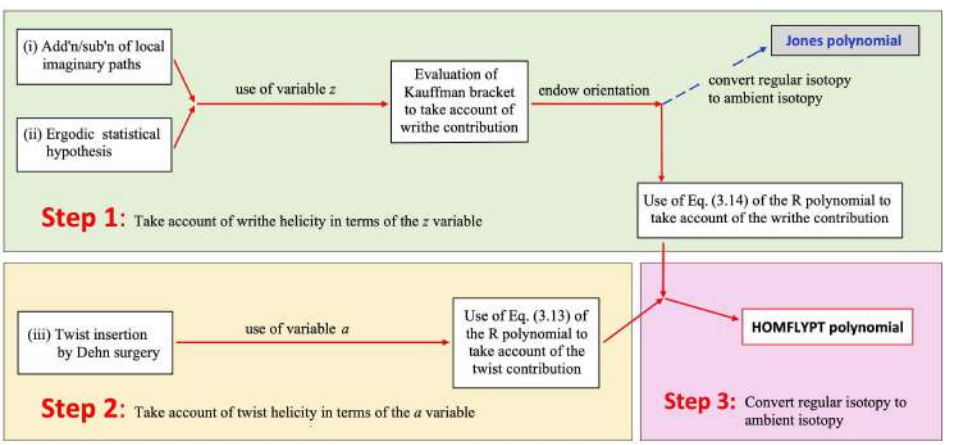

Fig. 8. Scheme of the proof of Theorem 3.3 according to [20].

that is

$$R\left(\uparrow \circlearrowleft\right) = \delta R\left(\uparrow\right) , \tag{30}$$

where $\delta = (a - a^{-1})/z$. By extending this equation to the knot diagram D, we get

$$R\left(D \circlearrowleft\right) = \delta R\left(D\right) , \tag{31}$$

which can be considered a supplementary rule for the derivation of the knot polynomial. The regular isotopy version of the HOMFLYPT with variables z and a specializes to a regular isotopy version of the Jones polynomial when $z = a - a^{-1}$. We make the physical heuristic that the variables a and z are independent of one another. Then these relations become relations for the HOMFLYPT polynomial, and this second stage is accomplished. For further details on these constructions, see [20].

The physical interpretation of the two variables is accomplished by taking $z = k - k^{-1}$, so that

$$k = \mathrm{e}^{2\lambda_\omega Wr}, \quad a = \mathrm{e}^{\lambda_\tau Tw}, \tag{32}$$

where $\lambda_\tau \in [0, 1]$ represents the uncertainty associated with twist; note that λ_ω and λ_τ are also totally independent from one another. Since reduction to Jones implies $ak^2 = 1$, from (32) we have

$$\lambda_\tau Tw = -2(2\lambda_\omega Wr) = -4\lambda_\omega Wr, \tag{33}$$

that gives a relation between writhe and twist, i.e. $Wr = -(\lambda_\tau/4\lambda_\omega)Tw$. As we did for the Jones polynomial, the adapted HOMFLYPT can now be computed by the numerical values obtained from $\langle Wr\rangle$ and $\langle Tw\rangle$, so that we can quantify the topology of physical knots and links by numerical values. For example, if we take the average values $\langle\lambda_\omega\rangle = \langle Wr\rangle = 1/2$, and $\langle\lambda_\tau\rangle = \langle Tw\rangle = 1/2$, we obtain

$$z = \mathrm{e}^{1/2} - \mathrm{e}^{-1/2} \approx 1.04, \quad a = \mathrm{e}^{1/4} \approx 1.28. \tag{34}$$

The table of Fig. 9 shows the computation of the adapted HOMFLYPT polynomial for the numerical values of a and z given by (34). A similar table for the adapted Jones polynomial [31] can evidently be obtained from the condition $ak^2 = 1$.

3.1. *A test case: Cascade of torus knots and links by adapted HOMFLYPT values*

Work done on vortex knot dynamics [16, 17, 38] shows that the evolution of torus knots is governed by a generic process of topological simplification, that gradually converts complex knots to simpler knots and unknots of ever decreasing smaller scales, towards final dissipation. The change of topology, due to a sequence of orientation-preserving reconnections induced by the local physics, generates a time-dependent pattern that can be exemplified by the topological cascade of torus knots and links $\{T(2, n)\}$ ($n \in \mathbb{N}$) shown in Fig. 10. Since the torus knots and links

Knot/link type	HOMFLYPT polynomial	Value
Single unknot	1	1
$N \geq 2$ unknots	$\delta^{N-1} = [(a - a^{-1})/z]^{N-1}$	0.48^{N-1}
Positive Hopf link	$a^{-1}z + \left(a^{-1} - a^{-3}\right) z^{-1}$	1.10
Negative Hopf link	$-az - \left(a - a^{3}\right) z^{-1}$	−0.54
Left-handed trefoil knot	$2a^2 + a^2z^2 - a^4$	2.36
Right-handed trefoil knot	$2a^{-2} + a^{-2}z^2 - a^{-4}$	1.51
Figure-of-8 knot	$a^{-2} - 1 - z^2 + a^2$	0.17
Withehead link	$-a^{-1}z^{-1} - a^{-1}z + az^{-1} + 2az + az^3 - a^3z$	1.59
Withehead link (mirror image)	$az^{-1} + az - a^{-1}z^{-1} - 2a^{-1}z - a^{-1}z^3 + a^{-3}z$	−0.20
Borromean rings	$a^{-2}z^{-2} - a^{-2}z^2 + a^2z^{-2} - a^2z^2 - 2z^{-2} + 2z^2 + z^4$	1.13

Fig. 9. HOMFLYPT polynomials and numerical values for some elementary oriented knots and links obtained by taking $a = 1.28$ and $z = 1.04$.

family admits representation in closed braid form, assuming reduction of topological complexity by a single reconnection event, we can apply the HOMFLYPT skein relation [15] in a recursive way to get the following result.

Theorem 3.4 ([20]). *Let us consider the family $\{T(2,n)\}$ of torus knots and links. The HOMFLYPT polynomial of $T(2,n)$ is given by*

$$P(T(2,n)) = \left[\frac{k^{n-2} - (-k)^{-(n-2)}}{a^{n-3}(k + k^{-1})}\right] P(T(2,3)) + \left[\frac{k^{n-3} - (-k)^{-(n-3)}}{a^{n-3}(k + k^{-1})}\right] P(T(2,2)), \tag{35}$$

where

$$P(T(2,3)) = 2a^{-2} + a^{-2}z^2 - a^{-4}, \quad P(T(2,2)) = a^{-1}z + (a^{-1} - a^{-3})z^{-1}. \tag{36}$$

For details of the proof, see [21, 31]. By relying on the information available from experiments, and applying the theory presented in the former section, we can compute the adapted HOMFLYPT polynomial $P(T(2,n))$ to quantify the sequence of fluid knots $\{T(2,n)\}$. Using the values given by (34) (with $k = \mathrm{e}^{1/2} \approx 1.65$) we obtain the results shown in Fig. 11. As we see, the numerical values form a

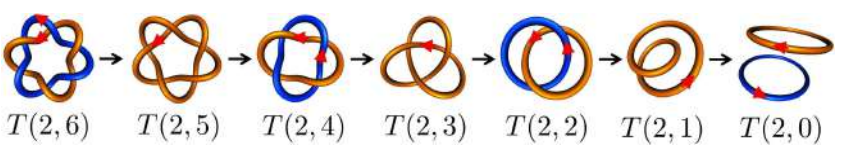

Fig. 10. Time sequence of topological transitions of torus knots and links by a single reconnection event, starting from the knot $T(2,6)$.

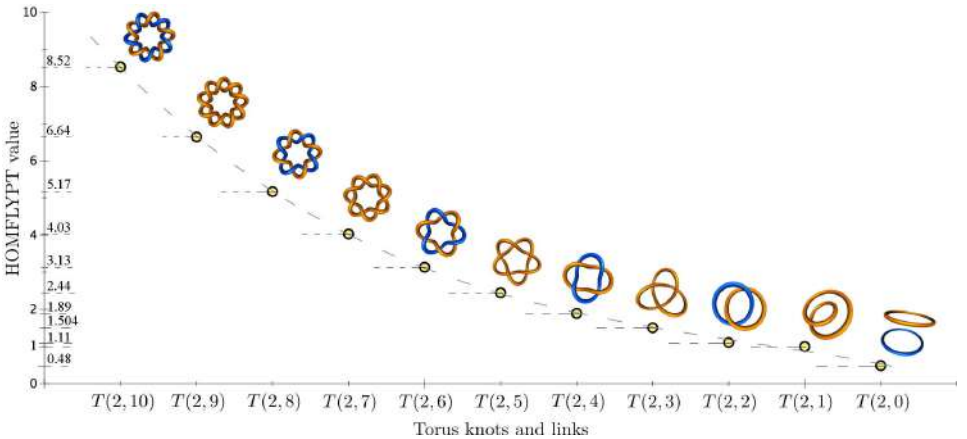

Fig. 11. HOMFLYPT values computed for the family of torus knots/links $\{T(2,n)\}$, $n = 0, 1, 2, \ldots, 10$.

monotonic decreasing sequence that is consistent with the observed topological cascade and the associated energy decay. Note that the same monotonic behavior is obtained by other (appropriate) different choice of numerical values, a fact rooted in the decreasing complexity of the original knot polynomials. A physical justification is given by considering the small, but non-zero reduction of the physical knot length due to the reconnection process, that produces the topological change. Since the kinetic energy of thin knots is proportional to the knot length, progressive shortening of the knot through topological simplification is often accompanied by a corresponding energy decrease. This correspondence is intriguing, and motivates the new approach to topological dynamics that is presented in the following section.

4. Jones Polynomials in Knot Polynomial Space

The adapted Jones polynomial introduced in Sec. 3 can be employed by defining a knot polynomial space to compute the untying pathways (seen as geodesics on this space) associated with the topological simplification of physical knots. For simplicity, let us confine the discussion to the subset of prime knots with $c_{\min} \leq 9$; for these knots the Jones polynomial has positive exponents of highest degree n, and it is in one-to-one correspondence with the given knot type. A knot polynomial space can thus be defined by a discrete set of points that represent the knot types considered through their Jones polynomials. We have [22].

Definition 4.1. The knot polynomial space $\mathcal{V}_n^+$ is an n-dimensional, discrete, Euclidean space endowed by an Euclidean metric, whose isolated points (singletons) are the adapted Jones polynomial $V(\mathcal{K})$ up to the degree n.

In order to compute the geodesics, we must endow $\mathcal{V}_n^+$ with a metric; since singletons are knot polynomials we can use orthogonal polynomials to construct

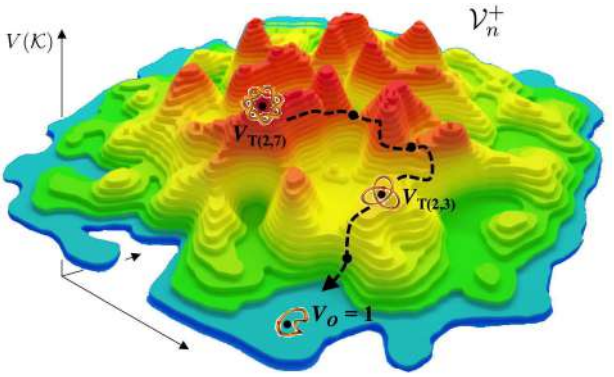

Fig. 12. A pictorial representation of the knot polynomial space $\mathcal{V}_n^+$, where each singleton (black dot) is represented by the knot given by its Jones polynomial. Height is given by the adapted Jones polynomial value according to $e^{\lambda_\omega} \in [1, e]$.

a suitable metric. The Legendre polynomials $\{P_n(x)\}$ of degree n, with weight function unity and inner product defined over the finite interval $[-1, 1]$, prove to be suitable to this end. These are given by

$$P_0(x) = 1, \quad P_1(x) = x, \quad P_2(x) = \frac{1}{2}(3x^2 - 1), \quad P_3(x) = \frac{1}{2}(5x^3 - 3x), \ldots,$$

with orthogonality condition given by

$$\langle P_n, P_m \rangle = \int_{-1}^{1} P_n(x) P_m(x) \mathrm{d}x = \frac{2}{2n+1} \delta_{nm}. \tag{37}$$

The unit-norm Legendre polynomial is thus defined by

$$L_n(x) = \sqrt{\frac{2n+1}{2}} P_n(x), \tag{38}$$

so that (37) becomes

$$\langle L_n, L_m \rangle = \int_{-1}^{1} L_n(x) L_m(x) \mathrm{d}x = \delta_{nm}. \tag{39}$$

This endows $\mathcal{V}_n^+$ with Euclidean metric. The following result can be proved [18].

Theorem 4.2. *A polynomial $V_n(x)$ of degree n can be expanded into the first $n+1$ Legendre polynomials $L_0(x)$, $L_1(x)$, …, $L_n(x)$ that provide a complete basis for the knot polynomial space $\mathcal{V}_n^+$.*

For physical applications (and for the sake of example) consider now the adapted Jones polynomial with $t^{1/2} = e^{2\lambda_\omega Wr}$, $\langle Wr \rangle = 1/2$, and $\lambda_\omega \in [0, 1]$. Taking $x = t^{1/2}$, we have $x = e^{\lambda_\omega} \in [1, e]$. In order to use (39), we must rescale the interval $[1, e]$ into

$[-1, 1]$ by the new variable x'

$$x' = \frac{2}{\mathrm{e}-1}x - \frac{1+\mathrm{e}}{\mathrm{e}-1}, \tag{40}$$

so that

$$\int_1^{\mathrm{e}} f[V_n(x)]\mathrm{d}x = \frac{2}{\mathrm{e}-1}\int_{-1}^{1} f[V(x')]\mathrm{d}x'. \tag{41}$$

Given the metric (39), we can now compute the coordinates of the knot $\mathcal{K}$ by identifying its adapted Jones polynomial $V(\mathcal{K})$ of degree n with the rescaled Legendre polynomial $V_n(x')$; we thus have

$$V(\mathcal{K}) = V_{\mathcal{K}}(x') = c_0 L_0(x') + c_1 L_1(x') + \cdots + c_n L_n(x'), \tag{42}$$

where the coordinates of $\mathcal{K}$ are given by

$$c_i = \int_{-1}^{1} V_{\mathcal{K}}(x') L_i(x')\mathrm{d}x' \quad (i = 0, \ldots, n). \tag{43}$$

The geodesic distance between the knots $\mathcal{K}_i$ and $\mathcal{K}_j$ can thus be defined as follows:

$$d(\mathcal{K}_i, \mathcal{K}_j) = \|V(\mathcal{K}_j) - V(\mathcal{K}_i)\| = \left[\frac{2}{\mathrm{e}-1}\int_{-1}^{1} (V_{\mathcal{K}_j}(x') - V_{\mathcal{K}_i}(x'))^2 \mathrm{d}x'\right]^{1/2}. \tag{44}$$

Let us identify the origin with the unknot O, so that $V_O = 1$ is the singleton value at the origin. The geodesic distance $d(\mathcal{K})$ of the knot $\mathcal{K}$ from the unknot O is thus given by

$$d(\mathcal{K}) = \|V_{\mathcal{K}} - 1\| = \left[\frac{2}{\mathrm{e}-1}\int_{-1}^{1} (V_{\mathcal{K}}(x') - 1)^2 \mathrm{d}x'\right]^{1/2}. \tag{45}$$

4.1. *Topological cascade by optimal pathways as geodesic flows in knot polynomial space*

The theory presented above can be applied to the case studied in [39]. For this we consider the various unlinking pathways that bring the torus knot $T(2, 6)$ to the unknot O (denoted by $T(2, 1)$) by successive, single, orientation-preserving reconnections that untie the initial knot in a stepwise manner, assuming that the process is governed by a continuous reduction of topological complexity. As shown by the diagrams of Fig. 13 we identify 11 knots/links and 17 different routes. By using the theory above we want to compute the probability associated with each unlinking pathway Π_i $(i = 1, \ldots, 17)$, and compare the results with those in [39], obtained by different methods. The coordinates of the 11 knots/links of the diagrams are computed using Eq. (43) (see [22, Table 1]); the 17 routes of the diagrams of Fig. 13

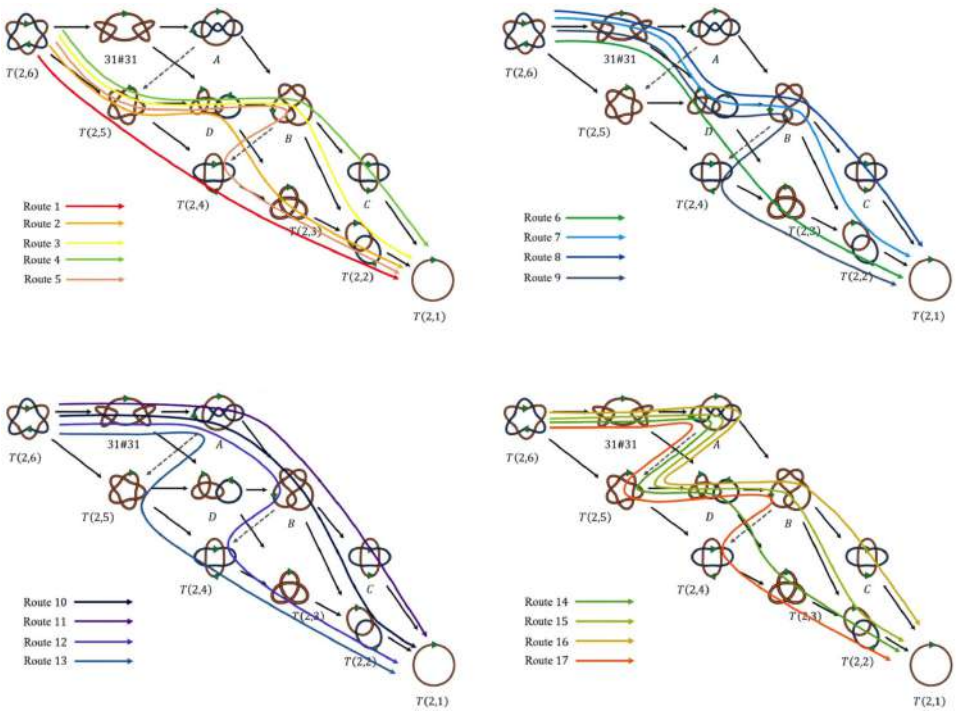

Fig. 13. (Color online) Diagrammatic representation of the 17 unlinking routes (different colors online) bringing the knot $T(2,6)$ to the unknot $T(2,1)$ by a sequence of single, orientation-preserving reconnections that simplify topological complexity in a stepwise manner (from [22]).

denote the 17 unlinking pathways, given by

$$\Pi_1: \quad T(2,6) \to T(2,5) \to T(2,4) \to T(2,3) \to T(2,2) \to T(2,1),$$

$$\Pi_2: \quad T(2,6) \to T(2,5) \to D \to T(2,2) \to T(2,1),$$

$$\Pi_3: \quad \ldots.$$

For each pathway Π_i, we compute the total length d_i given by the algebraic sum of the intermediate distances between knot types along Π_i; for example, for the path Π_1 we have

$$d_1 = d(T(2,6), T(2,5)) + d(T(2,5), T(2,4)) + \cdots + d(T(2,2), T(2,1)).$$

If we interpret the shortest path as the optimal route towards the unknot, pathway lengths can be related to the probability of occurrence by some simple definitions. For this let us define the 0-path by $\Pi_0 : T(2,6) \longrightarrow T(2,1)$, of length $d_0 = d\big(T(2,6), T(2,1)\big)$; the deviation of route Π_i from the 0-path Π_0 is given by

$$\sigma_i = \frac{d_i - d_0}{d_0}. \tag{46}$$

The probability associated with the occurrence of the pathway Π_i is thus defined by

$$p_i = \frac{\sigma_i^{-1}}{\sum_{i=1}^{17} \sigma_i^{-1}}, \tag{47}$$

which obviously satisfies the condition $\sum_{i=1}^{17} p_i = 1$. A direct computation for the pathway Π_1 shows that it has the smallest deviation $\sigma_1 = 2.68 \times 10^{-4}$, and the largest probability to occur $p_1 = 97.62\%$. It is interesting to note that the route Π_1 coincides with the sequence pictorially represented by Fig. 10. The monotonic decreasing sequence of the HOMFLYPT values is also consistent with the present computation based on the use of the adapted Jones polynomial. Route Π_{17} has the largest deviation $\sigma_{17} = 9.34 \times 10^{-1}$, and the smallest probability to occur $p_{17} = 2.80\%$. Direct comparison of probability values obtained by [39] and by the method presented here (see Fig. 14) shows very good agreement, and provides a convincing proof of the validity of the theory outlined above.

From (45) we can introduce a new definition of topological complexity of a knot $\mathcal{K}_i$ based on the distance $d(\mathcal{K}_i)$ [22].

Definition 4.3. The degree χ of topological complexity of a knot/link $\mathcal{K}$ is defined by

$$\chi(\mathcal{K}) = \ln(1 + d(\mathcal{K})). \tag{48}$$

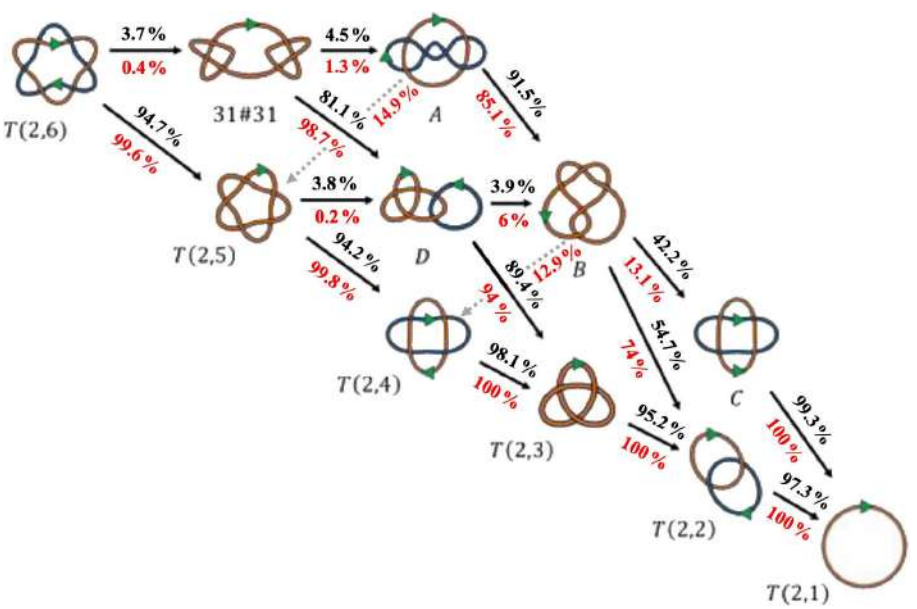

Fig. 14. Diagrammatic representation of the unlinking pathways bringing the knot $T(2,6)$ to the unknot $T(2,1)$. In black probability values associated with the topological transitions computed by the methods used by Stolz *et al.* [39]; in red probability values obtained by Eq. (47) (from [22]).

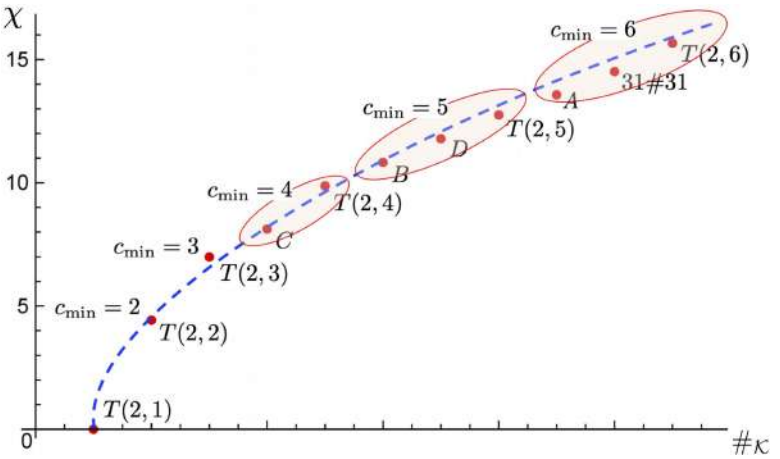

Fig. 15. (Color online) Complexity degree χ plotted against the 11 knots of the diagram of Fig. 14, listed according to the position $\#_{\mathcal{K}}$ tabulated according to their increasing ropelength. The dashed line (blue) is the best-fit curve given by Eq. (49). The knots/links with the same topological crossing number are grouped together in the highlighted regions.

Let us plot the values of $\chi = \chi(\#_{\mathcal{K}})$ against the 11 knots considered above (see Fig. 15), where $\#_{\mathcal{K}}$ is the position of the knot according to the increasing value of its ropelength [2, 7]. Knots/links with the same topological crossing number are grouped together in the highlighted regions. By interpolating these values with a best-fit curve, we find

$$\chi(\mathcal{K}) = 6.3 \ln \#_{\mathcal{K}} - 0.13. \tag{49}$$

The logarithmic behavior of the curve given by (49) is in good agreement with the logarithmic behavior of the ground state energy spectra of magnetic tight knots and links found by Ricca and Maggioni [32]. This is not surprising if we think that knot complexity, which grows with crossing number, is related to the minimum number of overpasses. Since knotted flux tubes are characterized by some physical thickness (say δ), each overpass length is at least $\pi\delta$ long. Since the energy of fluid knots is essentially proportional to the knot length, each reduction of crossing number must be accompanied by some small, but non-zero reduction of energy, due to a length decrease of (at least) $\pi\delta$. The minimum number of overpasses is therefore associated with some knot energy of strict topological nature. The minimum reconnection number $\aleph_r = c_{\min} - 1$ can thus be taken as a measure of the knot energy that either defines the ground state of a magnetic tight knot, or that can be absorbed by the dynamical untying of a fluid knot.

5. Conclusions

Kelvin's [40] vortex atom theory can be regarded as the first, true topological field theory (*ante litteram*), but real progress in topological fluid mechanics took

place only after the discovery of the conservation of helicity by Moreau in 1961, its topological interpretation in terms of linking numbers by Moffatt in 1968, and its application to vortex and magnetic fields that followed. In the quantum world, a similar progress was done in an extremely short period of time due to the revolutionary work of Witten in 1989, with the birth of topological quantum field theory. The discovery of the Jones [14] polynomials, and their interpretation in connection with the CS theory was essential for this progress. This proved useful for classical field theory as well. In analogy with the Wilson loops of CS theory, fluid knots of ideal fluid mechanics become the observables in an Abelian $U(1)$ theory, from which the Jones polynomials can be derived. With our work (done during the years 2012–2016) we have not only derived these polynomials from fluid helicity (vortex or magnetic), but by exploiting the fact that in classical field theory observables are measurable quantities (to any degree of accuracy!) we have also shown that (appropriately rescaled) the knot polynomials can be profitably used to assign numerical values to the topological complexity of knotted fields. This realization has gradually led people to look for the formation of knots [16, 23], and very complex ones have been discovered in superfluid turbulence [8], where vorticity is entirely localized on vortex lines. Since during evolution vortex knots reconnect undergoing by going through a topological simplification towards fully developed turbulence [17, 45], the intriguing question is to establish a relation between topological simplification and energy cascade. The new framework based on the knot polynomial space [22], where the untying pathways admit interpretation as geodesics on this space, seems a promising and powerful tool for this search. The results obtained so far by exploiting knot polynomial information are quite promising, suggesting that there is scope for further work in this direction.

Acknowledgments

R.L.R. wishes to acknowledge financial support from the National Natural Science Foundation of China (grant no. 11572005).

References

[1] V. I. Arnold and B. A. Khesin, *Topological Methods in Hydrodynamics* (Springer-Verlag, Berlin, 1998).
[2] T. Ashton, J. Cantarella, M. Piatek and E. Rawdon, Knot tightening by constrained gradient descent, *Exp Math.* **20** (2011) 57–90.
[3] C. F. Barenghi, R. L. Ricca and D. C. Samuels, How tangled is a tangle? *Physica D* **157** (2001) 197–206.
[4] M. A. Berger, An energy formula for nonlinear force-free magnetic fields, *Astron. Astrophys.* **201** (1988) 355–361.
[5] B. A. Berger and G. B. Field, The topological properties of magnetic helicity, *J. Fluid Mech.* **147** (1984) 133–148.
[6] G. Călugăreanu, Sur les classes d'isotopie des noeuds tridimensionnels et leurs invariants, *Czech Math J.* **11** (1961) 588–625.

[7] J. Cantarella, R. B. Kusner and J. M. Sullivan, On the minimum ropelength of knots and links, *Invent. Math.* **150** (2002) 257–286.
[8] R. G. Cooper, M. Mesgarnezhad, A. W. Baggaley and C. F. Barenghi, Knot spectrum of turbulence, *Sci. Rep.* **9** (2019) 10545.
[9] S. Coleman, *Aspects of Symmetry* (Cambridge University Press, Cambridge UK, 1985).
[10] S. Coleman, *Quantum Field Theory – Lectures of Sidney Coleman* (World Scientific, Singapore, 2019).
[11] Y.-S. Duan, X. Liu and P.-M. Zhang, Decomposition theory of the $U(1)$ gauge potential and the London assumption in topological quantum mechanics, *J. Phys., Cond. Matter* **14** (2002) 7941–7947.
[12] M. Elhamdadi, M. Hajij and K. Istvan, Framed knots, *Math. Intell.* **42** (2020) 7–22.
[13] P. Freyd, D. Yetter, J. Hoste, W. B. R. Lickorish and A. Ocneanu, A new polynomial invariant of knots and links, *Bull. Am. Math. Soc.* **12** (1985) 239–246.
[14] V. F. R. Jones, Hecke algebra representations of braid groups and link polynomials, *Ann. Math.* **126** (1987) 335–388.
[15] L. H. Kauffman, *On Knots* (Princeton University Press, Princeton, 1987).
[16] D. Kleckner and W. T. M. Irvine, Creation and dynamics of knotted vortices, *Nature Phys.* **9** (2013) 253–258.
[17] D. Kleckner, L. H. Kauffman and W. T. M. Irvine, How superfluid vortex knots untie, *Nature Phys.* **12** (2016) 650–655.
[18] S. Leon, *Linear Algebra with Applications* (Pearson, Prentice Hall, Upper Saddle River, 2010).
[19] X. Liu and R. L. Ricca, The Jones polynomial for fluid knots from helicity, *J. Phys. A, Math. Theor.* **45** (2012) 205501.
[20] X. Liu and R. L. Ricca, On the derivation of the HOMFLYPT polynomial invariant for fluid knots, *J. Fluid Mech.* **773** (2015) 34–48.
[21] X. Liu and R. L. Ricca, Knots cascade detected by a monotonically decreasing sequence of values, *Sci. Rep.* **6** (2016) 24118.
[22] X. Liu, R. L. Ricca and X.-F. Li, Minimal unlinking pathways as geodesics in knot polynomial space, *Commun. Phys.* **3** (2020) 136.
[23] M. Mesgarnezhad, R. G. Cooper, A. W. Baggaley and C. F. Barenghi, Helicity and topology of a small region of quantum vorticity, *Fluid Dyn. Res.* **50** (2018) 011403.
[24] H. K. Moffatt, The degree of knottedness of tangled vortex lines, *J. Fluid Mech.* **35** (1969) 117–129.
[25] H. K. Moffatt, Helicity and singular structures in fluid dynamics, *Proc. Natl. Acad. Sci. USA* **111** (2014) 3663–3670.
[26] H. K. Moffatt and R. L. Ricca, Helicity and the Călugăreanu invariant, *Proc. Roy. Soc. A* **439** (1992) 411–429.
[27] J. J. Moreau, Constantes d'un îlot tourbillonnaire en fluid parfait barotrope, *C. R. Acad. Sci. Paris* **252** (1961) 2810–2812.
[28] J. H. Przytycki and P. Traczyk, Conway algebras and skein equivalence of links, *Proc. Am. Math. Soc.* **100** (1987) 744–748.
[29] R. L. Ricca, Applications of knot theory in fluid mechanics, in *Knot Theory*, eds. V. F. R. Jones *et al.,* Vol. 42 (Knot Theory, Banach Center Publishers, Polish Academy of Sciences, Warsaw, 1998), pp. 321–346.
[30] R. L. Ricca and X. Liu, The Jones polynomial as a new invariant of topological fluid dynamics, *Fluid Dyn. Res.* **46** (2014) 061412.
[31] R. L. Ricca and X. Liu, HOMFLYPT polynomial is the best quantifier for topological cascades of vortex knots, *Fluid Dyn. Res.* **50** (2018) 011404.

[32] R. L. Ricca and F. Maggioni, On the groundstate energy spectrum of magnetic knots and links, *J. Phys. A, Math Theor* **47** (2014) 205501.
[33] R. L. Ricca and H. K. Moffatt, The helicity of a knotted vortex filament, in *Topological Aspects of the Dynamics of Fluids and Plasmas*, eds. H. K. Moffatt *et al.* (Kluwer Academic Publishers, Amsterdam, 1992), pp. 225–236.
[34] R. L. Ricca and B. Nipoti, Gauss' linking number revisited, *J. Knot Theory Ramif.* **20** (2011) 1325–1343.
[35] D. Rolfsen, *Knots and Links* (Publish or Perish, Berkeley CA, 1976).
[36] A. J. B. Russell, A. R. Yeates, G. Hornig and A. L. Wilmot-Smith, Evolution of field line helicity during magnetic reconnection, *Phys. Plasmas* **22** (2015) 032106.
[37] P. G. Saffman, *Vortex Dynamics* (Cambridge University Press, Cambridge, 1992).
[38] M. W. Scheeler, D. Kleckner, D. Proment, G. L. Kindlmann and W. T. M. Irvine, Helicity conservation by flow across scales in reconnecting vortex links and knots, *Proc. Natl. Acad. Sci. USA* **111** (2014) 15350–15355.
[39] R. Stolz, M. Yoshida, R. Brasher, K. Ishihara, D. J. Sherratt, K. Shimokawa and M. Vazquez, Pathways of DNA unlinking: A story of stepwise simplification, *Sci. Rep.* **7** (2017) 12420.
[40] W. Thomson (Lord Kelvin), On vortex motion, *Trans. Roy. Soc. Edin.* **25** (1868) 217–260.
[41] J. H. White, Self-linking and the Gauss integral in higher dimensions, *Am. J. Math.* **91** (1969) 693–728.
[42] G. W. Whitehead, A generalization of the Hopf invariant, *Proc. Natl. Acad. Sci. USA* **32** (1946) 188–190.
[43] E. Witten, Quantum field theory and the Jones polynomial, *Commun. Math. Phys.* **121** (1989) 351–399.
[44] S. Zuccher and R. L. Ricca, Relaxation of twist helicity in the cascade process of linked quantum vortices, *Phys. Rev. E* **95** (2017) 053109.
[45] S. Zuccher and R. L. Ricca, Creation of quantum knots and links driven by minimal surfaces, *J. Fluid Mech.* **942** (2022) A8.